Korean J. Chem. Eng., 39(4), 1065-1071 (2022)
DOI: 10.1007/s11814-021-0956-4

pISSN: 0256-1115
eISSN: 1975-7220

An effective method for cysteine determination based on fluorescence resonance energy system between co-doped graphene quantum dots and silver nanoparticles

Thi Hoa Le, Yong Nam Ahn, and Sang Joon Park†

Department of Chemical and Biological Engineering, Gachon University, Seongnam 13120, Korea
(*Received 12 August 2021 • Revised 2 September 2021 • Accepted 7 September 2021*)

Abstract−Cysteine (Cys) is a crucial amino acid. Developing a method for Cys evaluation and detection is necessary for the diagnosis of various diseases. A variety of sensors use graphene quantum dots (GQDs) for biological compound determination; however, GQDs demonstrate very poor fluorescence quantum yield. Therefore, we doped nitrogen and phosphorus into GQDs to form composite material NP-GQDs with enhanced fluorescence properties. NP-GQDs were characterized by ultraviolet-visible, fluorescence spectroscopy, transmission electron microscopy, and X-ray photoelectron spectroscopy. Then, we used NP-GQDs as donors and silver nanoparticles (AgNPs) as acceptors to design a fluorescence resonance energy transfer (FRET) system for Cys detection. Optimal conditions for sensing were investigated, and under these conditions our FRET system showed good results in Cys determination. The fluorescence intensity of NP-GQDs was quenched proportionally along with increasing Cys concentration from 0.5 to 4.5 μM and the limit of detection (LOD) was 0.1 μM. In the presence of different amino acids, the FRET system also showed excellent selectivity for the Cys detection.

Keywords: Silver Nanoparticles (AgNPs), Nitrogen-phosphorus Co-doped Graphene Quantum Dots (NP-GQDs), FRET System, Fluorescence Quenching, Cysteine

INTRODUCTION

Homocysteine (Hcy), cysteine (Cys), and glutathione (GSH) are biothiols which have attracted significant attention because of their crucial biological activity. Cys is a vital biothiol, playing a vital role in protein synthesis, detoxification, and diverse metabolic functions [1,2]. It is reported that 30-200 μM is a permissible range for free intracellular Cys concentrations [3,4], and a deficient or excess level is related to various diseases, including delayed growth, cancer, Parkinsonism, and arthritis [5-7]. Hence, the development of good methods for the Cys detection and Cys discrimination from other amino acids in biological systems is very necessary.

There are several reported methods for Cys detection, such as electrochemistry [8], colorimetry [9], and fluorescence [10-12]. The fluorescence approach is the most attractive and promising technique for Cys sensing because of its easy preparation, simple operation, fast response, sensitivity, and specificity. Moreover, fluorescent sensors allow the visualization of Cys in single cells, so they can be

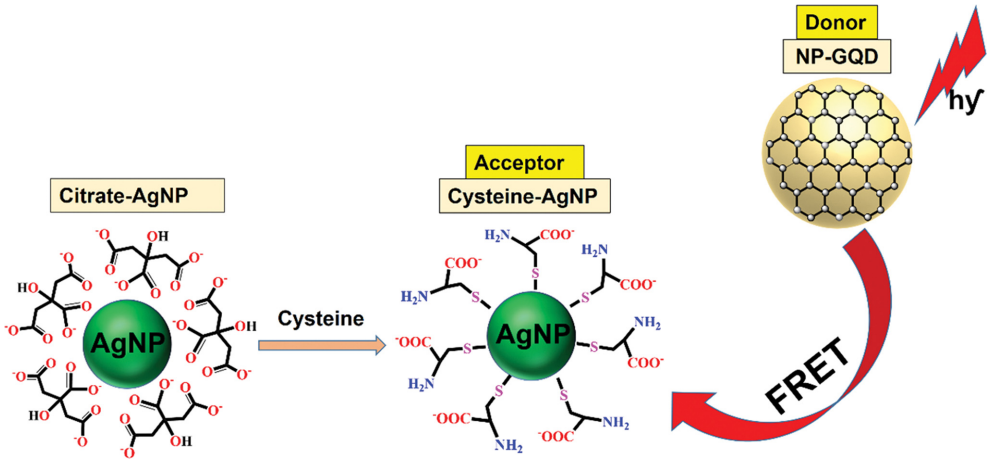

Scheme 1. FRET system between NP-GQDs and AgNPs for Cys detection.

†To whom correspondence should be addressed.
E-mail: psj@gachon.ac.kr

used widely in biological applications [13].

In our research, we developed a fluorescent sensor for Cys detection relying on the FRET process between NP-GQDs as donors and AgNPs as acceptors. GQDs are attracting much attention owing to distinct properties, for instance, favorable biocompatibility, cell membrane permeability, low toxicity, good solubility, tunable surface functionalities, and good photo-stability [14,15]. However, their low quantum yield (QY) limits their use in wider applications in fluorescent sensing [16,17]. Therefore, it is necessary to improve the fluorescent properties of GQDs. In our research, we used a hetero-doping method to enhance the fluorescent performance of GQDs. In particular, GQDs were doped with nitrogen (N) and phosphorus (P), and the results indicated that the fluorescent properties of GQDs increased significantly [18]. AgNPs have unique optical, electrical, and biological properties; therefore, they are widely used in many kinds of applications, including sensing [19]. Moreover, AgNPs were chosen to act as acceptors in our fluorescent sensor owing to their ability to interact with thiols such as Cys [20,21] to form a combination of AgNPs/Cys and then affect the FRET process from NP-GQDs to AgNPs. This is the basic mechanism for determining Cys using our FRET system (Scheme 1).

MATERIALS AND METHODS

1. Materials

All chemicals including $(NH_4)_2HPO_4$, $AgNO_3$, $Na_3C_6H_5O_7$, citric acid monohydrate, cysteine, glycine, tryptophan, lysine, glutamine, threonine, methionine, proline, and isoleucine, deionized (DI) water were obtained from Sigma-Aldrich.

2. Instruments and Measurements

Photoluminescence (PL) and UV-Vis spectra were conducted using a QuantaMaster TM 50 PTI spectrofluorometer from Photon Technology International, USA and a G1103A UV-Vis spectrophotometer (Agilent, USA) and. QY was measured using a FLUORO Q2100 device. Zeta potential measurements were obtained by electrophoretic light scattering (Photal Otsuka Electronics, ELS 8000). Transmission electron microscopy (TEM) was carried out using a FEI, Tecnai, F30S-Twin microscope. X-ray photoelectron spectroscopy (XPS) was performed using an X-ray photoelectron spectrometer (PHI 5000, Japan).

3. Synthesis of NP-GQDs

The fabrication of NP-GQDs was done using a hydrothermal technique. Five grams of $(NH_4)_2HPO_4$ and 2 g of citric acid monohydrate (molar ratio of 4 : 1) were added to 30 mL of DI water. Thereafter, transferring the mixture into a 50 mL Teflon-lined stainless steel autoclave and then heating at 180 °C during 4 h. A dark brown solution was obtained after cooling the autoclave. This solution was purified by filtering through a 0.22-μm polyethersulfone membrane, and next further dialyzed in a dialysis bag (MWCO: 1,000 Da). After 48 h, the obtained light violet colored solution was finally lyophilized to collect a powdery substance for later characterization. Undoped GQDs were fabricated following the same procedure without adding $(NH_4)_2HPO_4$.

4. Synthesis of AgNPs and Cys-stabilized AgNPs

AgNPs were synthesized using the Frens method [22]. $AgNO_3$ solution (50 mL, 0.001 M) was poured into an Erlenmeyer flask covered with aluminum foil and then heated to boiling. Next, 500 μL of 0.189 M trisodium citrate solution was dropped into the $AgNO_3$ solution under stirring. Then, this solution was heated until it began to boil. Then this product solution was centrifuged for 15 min at speed of 3,000 rpm. The precipitated product was washed and redispersed in DI water.

To prepare Cys-stabilized AgNPs, 10 μL Cys solution (125 μM) was added to 25 mL silver colloidal solution (5 nM). The solution was kept for 10 min in an orbital shaker for interaction between AgNPs and cysteine molecules.

5. Detection of Cys

For detecting Cys, a FRET system was established between AgNPs attached to Cys and NP-GQDs. First, varying amounts of Cys solution were added to a volume of AgNPs solution (3 nM) to obtain different concentrations (0, 0.5, 1, 1.5, 2, 2.5, 3, 3.5, 4, and 4.5 μM). The mixture was kept for 10 min. Then, 3 mL of NP-GQD suspension was added to the mixture. Afterward, the solution was diluted to the mark with DI water and keeping it in enquilibrium for 10 min to obtain the FRET system. Then, an excitation wavelength of 390 nm was used to measure the fluorescence intensity. Measuring at each concentration was carried out three times.

6. Selectivity Study

To study the specificity of this approach to Cys, the interference of other amino acids, including glycine, tryptophan, lysine, glutamine, threonine, methionine, proline, and isoleucine on the NP-GQDs/AgNPs system was investigated.

RESULTS AND DISCUSSION

1. NP-GQDs and AgNPs Characteristics

1-1. NP-GQDs

The XPS spectrum (Fig. 1) of NP-GQDs indicates that GQDs were successfully combined with N and P. The weight percentages were analyzed to be 30.23% (C), 11.93% (N), 48.98% (O) and 8.86% (P) (Fig. 1(a)). Fig. 1(b) demonstrates a deconvolution of C 1s peak. There are four peaks positioned at 284.5, 285.1, 286, and 289 eV, that are attributable to C-C/C=C, C-N/C-P, C-O, and C=O bonds, respectively, originating from the sp^2 graphitic structure [23] and several carboxyl, hydroxyl, amine, and phosphate groups on the surface of the NP-GQDs. With reference to the N 1s spectrum (Fig. 1(c)), the N 1s peak at 399.8 eV can be assigned to the N-H bond of an amine group or pyridinic N and the one located at 401.9 eV is assigned to graphitic N [24,25]. The P 2p spectrum (Fig. 1(d)) displays characteristic peaks at 134 and 135 eV, matching to P-O and P-C bonds.

The optical properties of NP-GQDs were characterized using fluorescence and UV-Vis absorption spectroscopy. Fig. 2(a) exhibits the absorption spectrum, which indicates a peak at 334 nm, which originates from the trapped excited state energy from the surface states [14,26,27].

In Fig. 2(b), GQDs and NP-GQDs reach the fluorescence emission peak at 452 nm and 440 nm, respectively, under the same excitation wavelength of 390 nm. Hence, there is a blue shift of the emission peaks after doping. Additionally, the intensity of the NP-GQDs is sharply enhanced compared to that of the GQDs alone. Furthermore, the NP-GQDs exhibited a QY of 76%, which is

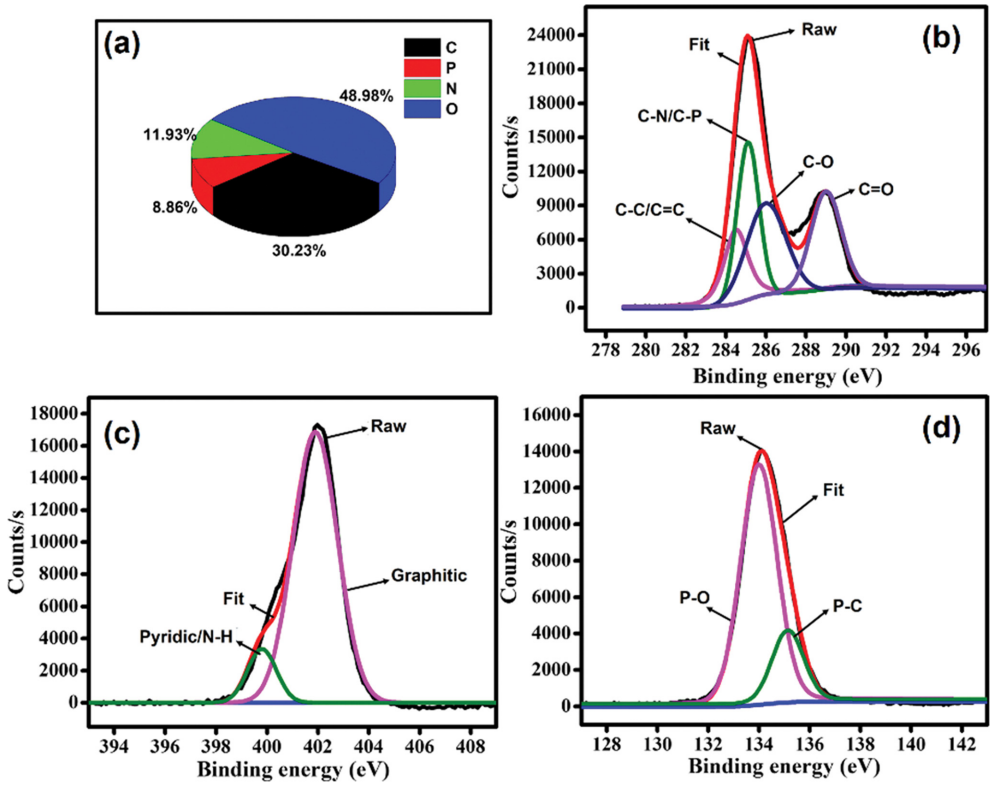

Fig. 1. Element weight percentage of NP-GQDs (a). High-resolution XPS spectra of (b) C 1s, (c) N 1s and (d) P 2p, respectively.

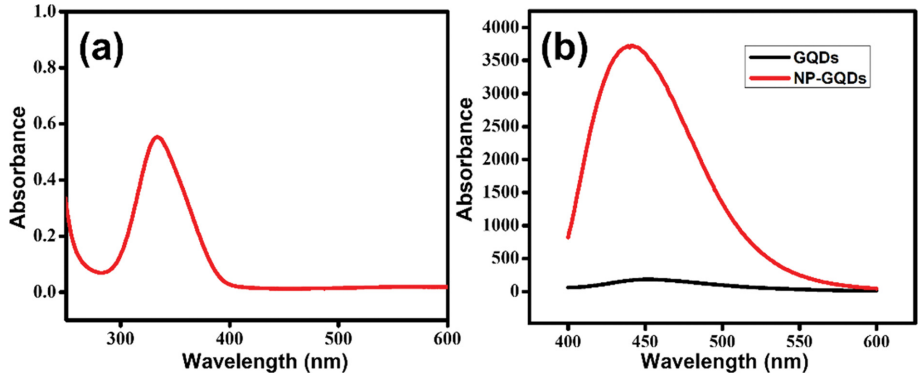

Fig. 2. (a) UV-Vis spectrum of NP-GQDs, (b) Photoluminescence spectra of GQDs and NP-GQDs.

approximately four times higher than that of undoped GQDs. This confirmed the effectiveness of N, P doping in enhancing the GQD fluorescence properties.

TEM images (Fig. 3(a)) show the morphology of the NP-GQDs. The size of NP-GQDs is distributed from 2.3 to 5.5 nm with an average value of 4.2 nm (Fig. 3(c)). The crystal structure of the NP-GQDs can be seen from the high-resolution (HRTEM) image (inset of Fig. 3(b)). A lattice parameter is determined of 0.157 nm, which is associated with graphitic diffraction planes [28].

1-2. AgNPs

Particle size strongly affects the optical properties of AgNPs. As can be seen in Fig. 3(d), AgNPs are multidisperse, with a broad size range of 23-70 nm. An absorption peak is observed for the AgNPs at 420 nm (Fig. 4).

2. Cys Attached to AgNPs (AgNPs/Cys)

Fig. 4 indicates that the addition of Cys into AgNP solution does not lead to a change in the location of the absorption peak. This confirms that there was no aggregation of the AgNPs after adding Cys.

To further study the interaction between AgNPs and Cys, experiments were carried out to measure zeta potential of the solutions. The AgNPs carried citrate ions, a strong negative charge ion so that the AgNP solution had a negative zeta potential value (−30.8 mV). The zeta potential value increased to −21.1 mV after adding 4 μM Cys. This confirms that trivalent citrate ions were exchanged with monovalent Cys anions. Then, Cys was adsorbed onto the AgNP

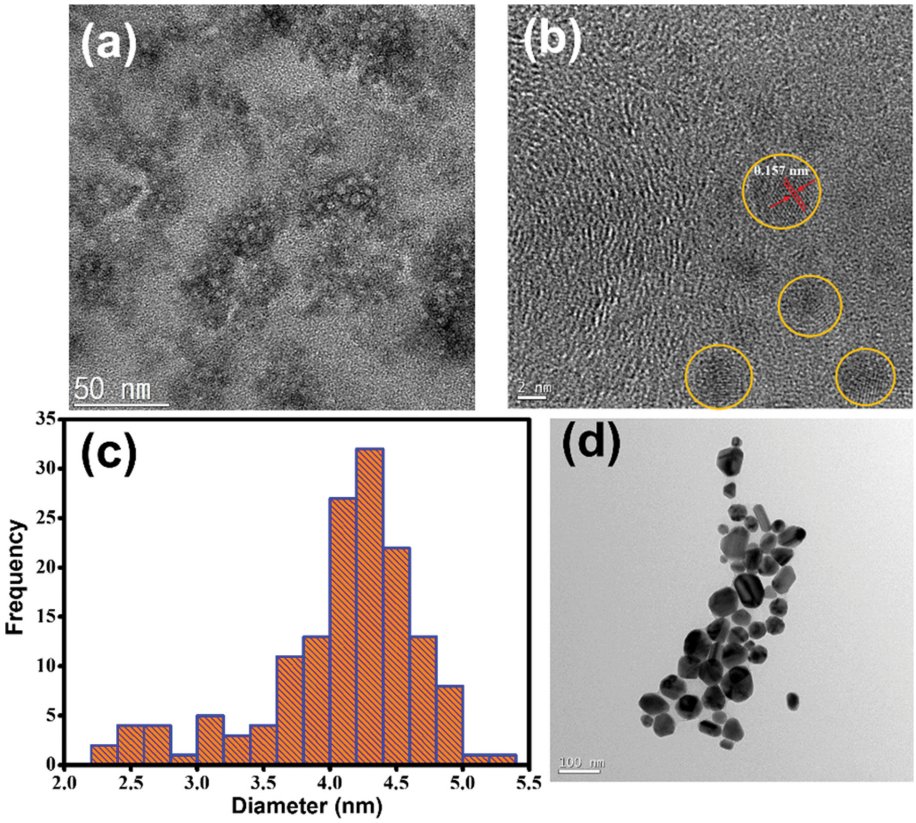

Fig. 3. (a) TEM image and (b) HRTEM image of NP-GQDs, (c) Size distribution of NP-GQDs, (d) TEM image of AgNPs.

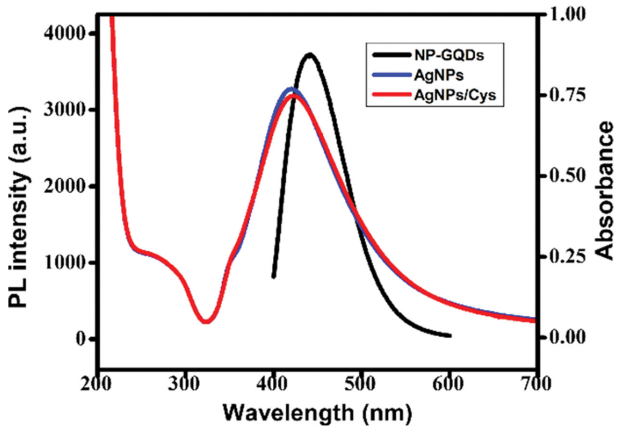

Fig. 4. The overlap between UV-Vis spectrum of AgNPs/Cys and photoluminescence emission spectrum of NP-GQDs.

surface and affected the surface charge of AgNPs (Scheme 1).

A mechanism is described to explain the exchange between citrate ions and Cys ions. Cys is a thiol amino acid. It is polar, with pKa values of 10.28, 8.18, 1.96 for thiol, amine, and carboxyl group, respectively. The isoelectric pH of Cys is 5.07. The synthesized AgNP solution has pH of 6.5. The functional groups of Cys are protonated at this pH. Therefore, the thiol groups of Cys can bind to the silver surface by ligand exchange reactions [29]. The link between Cys and AgNPs is described in Scheme 1.

3. FRET System between NP-GQDs and AgNPs/Cys

The most important step for the FRET process is the selection of suitable donor and acceptor substances. NP-GQDs, which have excellent fluorescence properties with a high QY, are ideal donor chromophores. Moreover, NP-GQDs are completely safe for various biomedical and environmental applications. AgNPs are widely used in pharmaceuticals and biosensors because of their low toxicity, good biocompatibility, good stability, high extinction coefficient, strong surface plasmon resonance, and distance-dependent optical properties [30,31]. The FRET process between NP-GQDs and AgNPs/Cys can occur if there is an appropriate overlap between their absorption and emission spectra. Fig. 4 indicates that the maximum fluorescence emission peak of NP-GQDs significantly overlaps with the maximum absorption peak of AgNPs/Cys. Therefore, energy can be transferred from NP-GQDs donors to AgNPs/Cys acceptors, which leads to a quenching in fluorescence intensity of NP-GQDs.

4. Cys Detection

4-1. Optimized Concentration of AgNPs Attached to Cys

To determine the optimal concentration of AgNPs, we assumed that (1) all Cys molecules attached to the AgNPs formed a FRET system with NP-GQDs, and (2) free NP-GQDs were not present in the solution. In this case, the amount of AgNPs remained unchanged and the fluorescence intensity of NP-GQDs was well turned off. If the concentration of NP-GQDs exceeds the desired concentration, the fluorescence emission spectrum of a small amount of free NP-GQDs is not quenched because of the signal from the

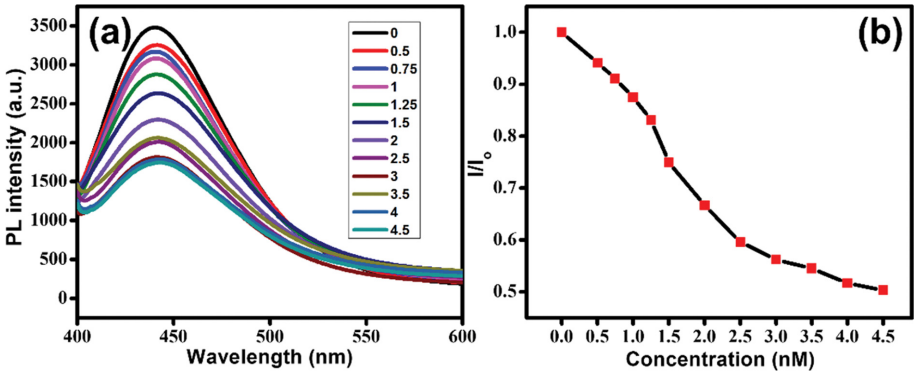

Fig. 5. (a) Fluorescence emission spectra of NP-GQDs during FRET process with various concentrations of AgNPs attached to Cys (4 μM). (b) Variation of I/I_0 ratio in the presence of Cys (4 μM) with different amounts of AgNPs.

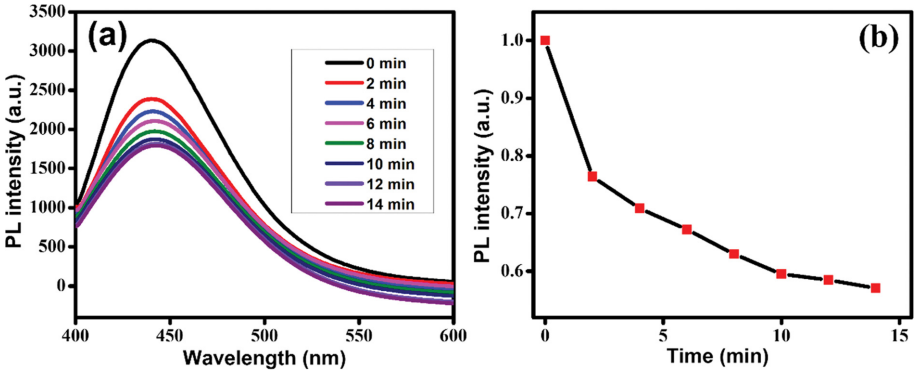

Fig. 6. (a) Fluorescence intensity of NP-GQD, (b) Variation of I/I_0 over time with concentrations of AgNPs: 3 nM and Cys: 3.5 μM.

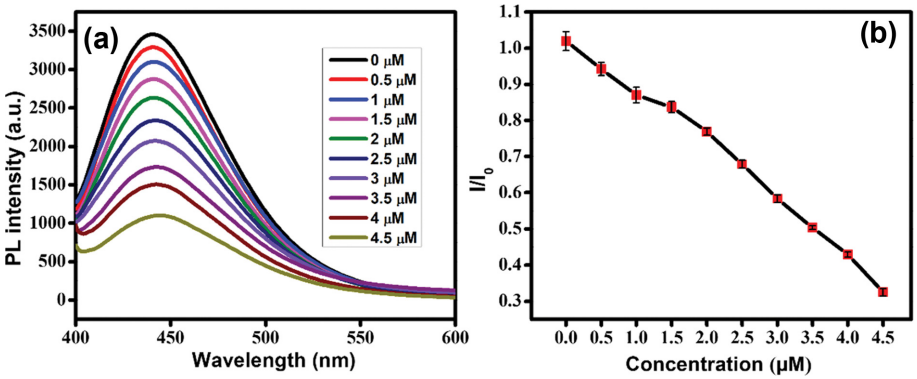

Fig. 7. (a) Fluorescence spectra of NP-GQDs in existence of various C_M of Cys, and (b) linear relationship between I/I_0 and Cys C_M.

control solution. A variety of concentrations of AgNPs attached to a fixed amount of Cys (4 μM) were studied through the formation of a FRET system with NP-GQDs. The fluorescence intensity of NP-GQDs was measured by increasing the AgNP concentration from 0.5 to 4.5 nM. As can be seen from Fig. 5, with an increase in the AgNP concentration attached to the same amount of Cys, the fluorescence intensity of NP-GQDs decreases because a FRET system is formed and progresses. The intensity continuously decreases with AgNP concentration from 0.5 to 3 nM, and a further increase does not cause a significant change in fluorescence intensity. Hence, 3 nM is the optimal concentration of AgNPs to attach to Cys.

4-2. Kinetics of NP-GQDs and AgNPs/Cys FRET System

After adding 3 nM AgNPs to a fixed amount of Cys and NP-GQDs system, time scanning was performed to investigate the kinetics of FRET system formation. The fluorescence intensity was recorded every 2 min (Fig. 6). After 10 min, the intensity dropped to the lowest level and remained quite stable. Therefore, 10 min was chosen as the optimal time for the next step.

4-3. Detection of Cys

Fig. 7 clearly shows fluorescence quenching of the NP-GQDs in the presence of AgNPs/Cys. Because the FRET process progresses

Table 1. The comparison of the Cys detection results of our method to the reported methods

Linear range	LOD	Method
	0.1 μM	[32]
	0.12 μM	[33]
1-888 μM	0.1 μM	[34]
1-10 μM	0.15 μM	[35]
0.5-832.5 μM	0.1 μM	[36]
0.5-10 μM	0.03 μM	[37]
0.5-4.5 μM	0.1 μM	Our method

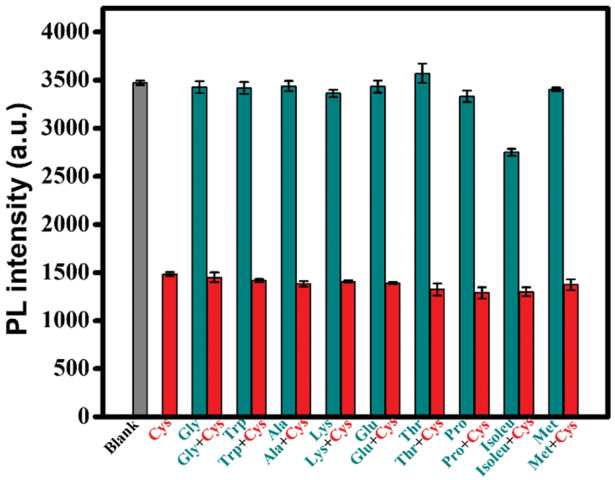

Fig. 8. Selectivity of NP-GQDs probe toward different amino acid in the presence and absence of Cys (5 μM).

between NP-GQDs and AgNPs/Cys, the intensity of NP-GQDs declines steadily when Cys level is increased (Fig. 7). When the Cys concentration is within the range 0.5-4.5 μM, the calibration curve between the relative NP-GQDs intensity and Cys concentration displays a good linear relationship with the quenching equation, that is, I/I_0=1.06318-0.15957 C_M, with a correlation coefficient (R^2) value of 0.99076. The measuring was carried out three times and the data were plotted with standard deviations. In addition, the LOD value was determined to be approximately 0.1 μM. A comparison of the detection results using our approach with those of other approaches is shown in Table 1.

5. Selectivity

Specificity is one of the most important factors for evaluating a sensor. To verify whether the presented sensor is specific for Cys detection, the fluorescent response in existence of other amino acids was investigated. Fig. 8 indicates that the quenching effect of Cys is much more considerable than that of other substances. This confirms that our FRET system exhibits excellent selectivity for detecting Cys.

CONCLUSION

We successfully designed a FRET system for the Cys sensing based on NP-GQDs and AgNPs. NP-GQDs have outstanding fluorescence properties in comparison to those of traditional GQDs and act as effective donors. AgNPs play an important role as acceptors, and the interaction between AgNPs and Cys has an increasing quenching effect on the fluorescence intensity of NP-GQDs; this was used as the basic principle for Cys detection. The fluorescence of NP-GQDs decreases steadily along with increasing in the level of Cys, and a linear response was obtained for Cys concentration from 0.5 to 4.5 μM and LOD value of 0.1 μM. The FRET system also shows good selectivity to Cys in presence of different amino acids. Therefore, with its features such as low cost, simple design, selectivity, and sensitivity, the sensor studied in this research can contribute to developing a strategy for other biomedical applications.

ACKNOWLEDGEMENTS

This research was supported by the Basic Science Capacity Enhancement Project through Korea Basic Science Institute (National research Facilities and Equipment Center) grant funded by the Ministry of Education (Grant No. 2019R1A6C1010016).

REFERENCES

1. J. Cao, X. Jiang and N. Fu, *Dyes Pigm.*, **174**, 107978 (2020).
2. Y. Wang, Q. T. Meng, Q. Han, G. J. He, Y. Y. Hu, H. Feng, H. M. Jia, R. Zhang and Z. Q. Zhang, *New J. Chem.*, **42**, 15839 (2018).
3. M. Qian, J. Xia, L. W. Zhang, Q. X. Chen, J. L. Guo, H. Y. Cui, Y. S. Kafuti, J. Y. Wang and X J. Peng, *Sens. Actuator B-Chem.*, **321**, 128441 (2020).
4. E. Weerapana, C. Wang, G. M. Simon, F. Richter, S. Khare, M. B. D. Dillon, D. A. Bachovchin, K. Mowen, D. Baker and B. F. Cravatt, *Nature*, **468**, 790 (2010).
5. T. K. Chung, M. A. Funk and D. H. Baker, *J. Nutr.*, **120**, 158 (1990).
6. X. X. Xie, C. X. Yin, Y. K. Yue and F. J. Huo, *Sens. Actuator B-Chem.*, **267**, 76 (2018).
7. S. Shahrokhian, *Anal. Chem.*, **73**, 5972 (2001).
8. S. L. Yang, G. Li, N. Xia, Y. X. Wang, P. P. Liu and L. B. Qu, *J. Alloys Compd.*, **853**, 157077 (2021).
9. S. Sahu, S. Sharma, T. Kant, K. Shrivas and K. K. Ghosh, *Spectroc. Acta Pt. A-Molec. Biomolec. Spectr.*, **246**, 118961 (2021).
10. X. F. Hou, Z. S. Li, Y. Q. Li, Q. H. Zhou, C. H. Liu, D. Fan, J. J. Wang, R. J. Xu and Z. H. Xu, *Spectroc. Acta Pt. A-Molec. Biomolec. Spectr.*, **246**, 119030 (2021).
11. J. X. Hong and G. Q. Feng, *Sens. Actuator B-Chem.*, **326**, 129016 (2021).
12. B. Feng, Y. Liu, S. Huang, X. Y. Huang, L. Huang, M. Liu, J. X. Wu, T. Du, S. L. Wang, X. P. Feng and W. B. Zeng, *Sens. Actuator B-Chem.*, **325**, 128786 (2020).
13. J. Shi, Y. Wang, X. Tang, W. Liu, H. Jiang, W. Dou and W. Liu, *Dyes Pigm.*, **100**, 255 (2014).
14. F. L. Ming, J. Z. Hou, C. J. Hou, M. Yang, X. F. Wang, J. W. Li, D. Q. Huo and Q. He, *Spectroc. Acta Pt. A-Molec. Biomolec. Spectr.*, **222**, 8 (2019).
15. X. R. Wu, L. N. Wu, X. Z. Cao, Y. Li, A. R. Liu and S. Q. Liu, *RSC Adv.*, **8**, 20000 (2018).
16. L. P. Lin, Y. H. Wang, Y. L. Xiao and W. Liu, *Microchim. Acta*, **186**, 7 (2019).

17. Y. T. Xie, J. X. Zheng, Y. L. Wang, J. L. Wan, Y. Z. Yang, X. G. Liu and Y. K. Chen, *Nanotechnology*, **30**, 10 (2019).
18. T. H. Le, H. J. Lee, J. H. Kim and S. J. Park, *Sensors*, **20**, 3470 (2020).
19. J. K. Daniels and G. Chumanov, *J. Electroanal. Chem.*, **575**, 203 (2005).
20. H. S. Jiang, Y. Zhang, Z. W. Lu, R. Lebrun, B. Gontero and W. Li, *Small*, **15**, e1900860 (2019).
21. Á. I. López-Lorente, M. L. Soriano and M. Valcárcel, *Microchim. Acta*, **181**, 1789 (2014).
22. M. Gakiya-Teruya, L. Palomino-Marcelo and J. C. F. Rodriguez-Reyes, *Methods Protoc.*, **2**, 3 (2019).
23. Q. Xu, B. F. Li, Y. C. Ye, W. Cai, W. J. Li, C. Y. Yang, Y. S. Chen, M. Xu, N. Li, X. S. Zheng, J. Street, Y. Luo and L. L. Cai, *Nano Res.*, **11**, 3691 (2018).
24. Y. Xu, M. Wu, Y. Liu, X. Z. Feng, X. B. Yin, X. W. He and Y. K. Zhang, *Chem. Eur. J.*, **19**, 2276 (2013).
25. S. Liu, J. Q. Tian, L. Wang, Y. W. Zhang, X. Y. Qin, Y. L. Luo, A. M. Asiri, A. O. Al-Youbi and X. P. Sun, *Adv. Mater.*, **24**, 2037 (2012).
26. M. Amjadi, T. Hallaj, J. L. Manzoori and T. Shahbazsaghir, *Spectroc. Acta Pt. A-Molec. Biomolec. Spectr.*, **201**, 223 (2018).
27. W. J. Wang, J. W. Peng, F. M. Li, B. Y. Su, X. Chen and X. M. Chen, *Microchim. Acta*, **186**, 32 (2019)
28. D. Qu, Z. C. Sun, M. Zheng, J. Li, Y. Q. Zhang, G. Q. Zhang, H. F. Zhao, X. Y. Liu and Z. G. Xie, *Adv. Opt. Mater.*, **3**, 360 (2015).
29. S. Aryal, K. C. R. Bahadur, N. Bhattarai, C. K. Kim and H. Y. Kim, *J. Colloid Interface Sci.*, **299**, 189 (2006).
30. Z. G. Shen, G. C. Han, C. F. Liu, X. Y. Wang and R. C. Sun, *J. Alloys Compd.*, **686**, 82 (2016).
31. M. L. Yola, V. K. Gupta, T. Eren, A. E. Sen and N. Atar, *Electrochim. Acta*, **120**, 204 (2014).
32. M. Hussain, N. Khaliq, A. Nisar, M. Khan, S. Karim, A. A. Khan, X. Yi, M. Maqbool and G. Ali, *Nanotechnology*, **31**, 13 (2020).
33. Y. T. Yu, J. B. Wang, H. Xiang, L. K. Ying, C. Y. Wu, H. W. Zhou and H. Y. Liu, *Dyes Pigm.*, **183**, 7 (2020).
34. L. Yang, G. Li, N. Xia, Y. X. Wang, P. P. Liu and L. B. Qu, *J. Alloys Compd.*, **853**, 9 (2021).
35. Y. M. Zhang, J. Song, W. H. Shao and J. Li, *Micropor. Mesopor. Mater.*, **310**, 9 (2021).
36. S. L. Yang, G. Li, N. Xia, P. P. Liu, Y. X. Wang and L. B. Qu, *J. Electroanal. Chem.*, **877**, 9 (2020).
37. N. Vladislavic, I. S. Roncevic, M. Buzuk, M. Buljac and I. Drventic, *J. Solid State Electrochem.*, **25**, 841 (2021).